

Valorization of Oil Palm Empty Fruit Bunches into Sulfonated Carbon Catalysts for Esterification of Vegetable Oil

Gimelliya Saragih^{1*}, Vivi Purwandari², Nelson Silitonga³, Abdillah⁴, Yenny Sitanggang⁵, Liver Zai⁶, Mukhtissiani⁷

^{1,5}Department of Chemical Engineering, Politeknik Teknologi Kimia Industri, Jl. Medan Tenggara VII, Medan 20228, Indonesia

^{2,6,7}Department of Chemistry, Universitas Sari Mutiara Indonesia, Jalan Kapten Muslim No.79, Medan 20123, Indonesia

^{3,4}Department of Mechanical Engineering, Politeknik Teknologi Kimia Industri, Jl. Medan Tenggara VII, Medan 20228, Indonesia

Abstract

This study reports the synthesis, characterization, and catalytic evaluation of sulfonated carbon derived from oil palm empty fruit bunches (OPEFB) for biodiesel production. Activated carbon produced through controlled pyrolysis was sulfonated using sulfuric acid concentrations of 7%, 10%, and 13% to examine the influence of acid strength on catalyst properties. The materials were characterized using TGA/DTA, FTIR, BET, and SEM to assess thermal stability, functional group incorporation, surface morphology, and porosity. Among the prepared samples, the catalyst treated with 10% H₂SO₄ (SA-10) exhibited the most favorable combination of surface area, pore accessibility, and -SO₃H density. Esterification of waste cooking oil (WCO) at 65 °C for 2 h demonstrated that SA-10 achieved the highest ester yield (43.28%) at a catalyst loading of 3 g, outperforming samples with insufficient or excessive sulfonation. These findings highlight the potential of OPEFB as a sustainable precursor for solid acid catalyst development and emphasize the importance of optimizing sulfonation conditions to enhance catalytic performance. Further studies on catalyst reusability, kinetic behavior, and techno-economic feasibility are recommended to support industrial-scale application.

Keywords: Esterification; Functional material; Heterogeneous catalyst; Sulfonated carbon

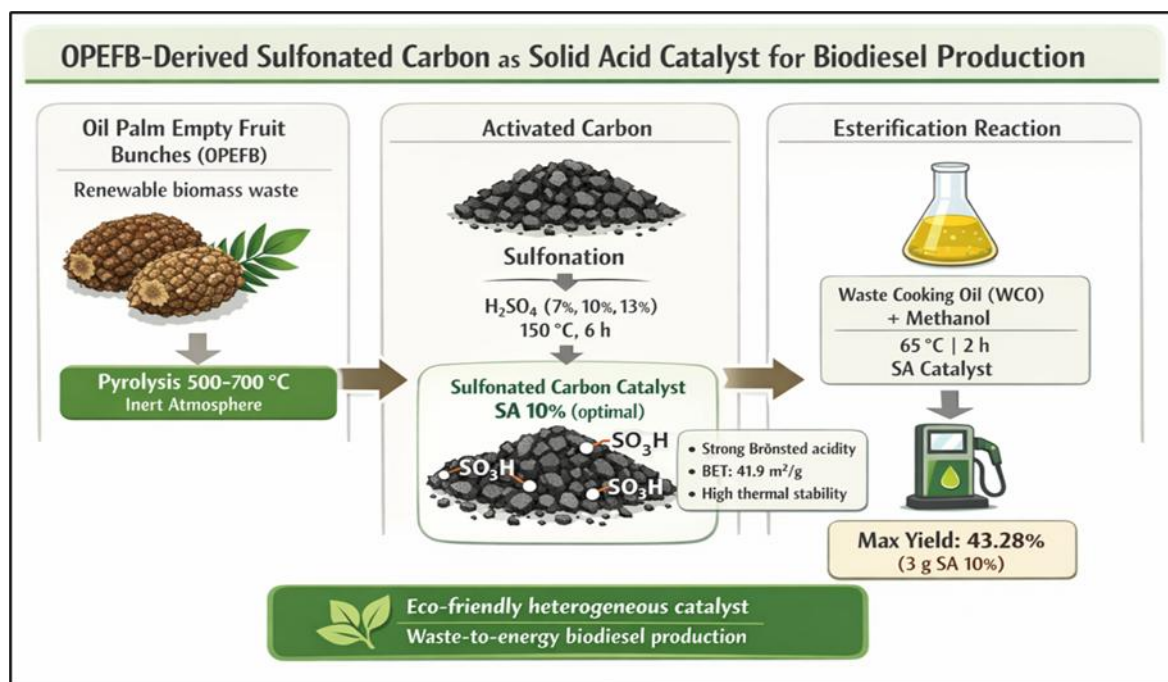
* Corresponding author
Email address: gimelliya@ptki.ac.id

DOI: <https://doi.org/10.22437/chp.v9i2.47630>

Received August 05th 2025; Accepted November 25th 2025; Available online December 19th 2025

Copyright © 2025 by Authors, Published by Chempublish Journal. This is an open access article under the CC BY License (<https://creativecommons.org/licenses/by/4.0>)

Graphical Abstract



Introduction

Growing concerns over environmental degradation and the depletion of fossil-based resources have accelerated the development of renewable energy technologies [1–2]. Biodiesel, derived from biomass-based materials, has received considerable attention as a biodegradable and environmentally sustainable substitute for petroleum-derived diesel [3–5]. Waste cooking oil (WCO), in particular, is an abundant and low-cost feedstock [6–8] with a high free fatty acid (FFA) content, offering both economic benefits and opportunities for sustainable waste valorization [9–10].

Traditional esterification processes commonly employ homogeneous acid catalysts such as sulfuric acid; however, their use is associated with several drawbacks, including complex catalyst separation, equipment corrosion, and adverse environmental impacts [11–13]. As a result, heterogeneous solid acid catalysts have emerged as more sustainable alternatives [14–15]. Among them, sulfonated carbon-

based catalysts have shown notable promise due to their strong Brønsted acidity, thermal stability, and reusability, as highlighted by Chong et al. (2021) [16].

Agricultural residues such as oil palm empty fruit bunches (OPEFB) represent attractive precursors for carbon-based catalysts owing to their high carbon content [17], intrinsic porosity [18], and wide availability in palm-oil-producing regions [19]. Controlled pyrolysis of OPEFB produces activated carbon with favorable structural characteristics [20–22], while subsequent sulfonation using sulfuric acid introduces $-\text{SO}_3\text{H}$ groups that impart strong acidity suitable for esterification reactions [23–24].

The physicochemical characteristics of sulfonated carbon—including surface area, thermal stability, pore morphology, and acid site density—are strongly influenced by the sulfonation conditions and the chemical nature of the precursor [25–26]. Although earlier studies have examined the sulfonation of various biomass sources such as glucose, starch, and lignocellulosic

materials [27–28], systematic investigations specifically targeting OPEFB-derived sulfonated carbon remain limited. In particular, there is a lack of comprehensive studies evaluating how variations in sulfuric acid concentration influence both the structural attributes of the catalyst and its catalytic performance.

To address this gap, the present work synthesizes sulfonated carbon catalysts from OPEFB using controlled sulfuric acid concentrations (7%, 10%, and 13%) and evaluates their catalytic performance in the esterification of waste cooking oil (WCO) under mild reaction conditions. The novelty of this study lies in the utilization of OPEFB as a sustainable precursor, the application of mild sulfonation strategies, and a systematic assessment that links physicochemical properties to catalytic behavior. This study offers new insights into the relationship between sulfonation degree, catalyst structure, and biodiesel yield, thereby addressing an important gap in the existing literature.

Materials and Methods

Synthesis of Carbon Material from Oil Palm Biomass (OPEFB)

OPEFB obtained from PT. Gergas Utama, Langkat was first washed to remove dirt and impurities and then sun-dried. The dried biomass was further dehydrated in an oven at 105 °C for 24 h to eliminate residual bound moisture. The dried and shredded OPEFB was subsequently subjected to pyrolysis at 500–700 °C [27] for a fixed residence time of 2 h [28], a duration selected to ensure adequate carbonization and promote stable pore development without inducing structural collapse. The resulting activated carbon was allowed to

cool naturally to room temperature and was stored in a desiccator prior to use.

Sulfonation of Activated Carbon.

Activated carbon produced from pyrolysis was sulfonated using sulfuric acid solutions of 7%, 10%, and 13% (w/w), prepared by diluting concentrated H₂SO₄ (98%) with deionized water. A carbon-to-acid mass ratio of 1:10 was applied. The mixture was placed in a 250-mL three-neck round-bottom flask equipped with a reflux condenser and positioned in a temperature-controlled oil bath inside a fume hood to ensure safe handling of potential SO₂ vapors. The reaction system remained closed but not pressurized to minimize acid loss during heating.

Sulfonation was performed at 150 °C for 6 h under continuous magnetic stirring (400 rpm) to ensure uniform interaction between the carbon matrix and the acid. After completion, the mixture was cooled to room temperature, washed repeatedly with deionized water until neutral pH was achieved, and dried at 105 °C for 24 h.

For clarity, samples are labeled according to their treatment conditions. CA denotes the activated carbon obtained from pyrolysis without sulfonation. SA-7, SA-10, and SA-13 represent carbon sulfonated with 7%, 10%, and 13% H₂SO₄, respectively. These materials were subjected to thermal, structural, and morphological characterization (TGA/DTA, FTIR, BET, and SEM) to assess the influence of sulfonation conditions on their physicochemical properties.

Esterification Procedure.

Esterification was conducted using waste cooking oil (WCO) as the feedstock. The WCO was weighed, placed in a three-neck flask equipped with a condenser, and preheated

to 65 °C to avoid methanol evaporation. Methanol was added according to the predetermined stoichiometric ratio, followed by the addition of the sulfonated carbon catalyst (0 g, 3 g, or 5 g depending on the experiment).

The reaction mixture was refluxed at 65 °C for 2 h under continuous magnetic stirring. This reaction time is widely reported as sufficient for effective esterification and to promote proper mass transfer among methanol, the oil phase, and the solid catalyst. Maintaining stirring throughout the reaction also prevents catalyst settling and enhances catalytic contact, thereby improving conversion efficiency [11].

After reaction, the mixture was allowed to settle into two layers: an upper biodiesel layer and a lower glycerin-rich phase containing residual catalyst. The biodiesel layer was separated using a separatory funnel, washed with warm water to remove remaining methanol and catalyst residues, and dried using anhydrous sodium sulfate (Na_2SO_4). The final biodiesel product was analyzed by FTIR to confirm ester functional group formation.

Characterization Techniques.

Comprehensive characterization was performed on both activated and sulfonated carbon samples. FTIR spectra were recorded using a Shimadzu IR-Prestige 21 spectrophotometer to identify characteristic functional groups, particularly to confirm the presence of $-\text{SO}_3\text{H}$ functionalities and to verify ester formation in biodiesel. Surface morphology was examined using SEM imaging with a Bruker instrument. Surface area and porosity were evaluated through BET analysis using a Quantachrome system. Thermal stability and decomposition behavior were assessed using TGA/DTA with an STA TG/DTA 7300 analyzer.

Result and Discussion

As the WCO was used in its as-received condition, its composition likely reflects the typical characteristics of recycled frying oils reported in the literature. Such oils commonly contain 3–15% free fatty acids (FFA), which promote water formation during esterification and subsequently shift the reaction equilibrium toward the reactants under mild conditions. Residual moisture content generally 0.2–1.5% further suppresses ester conversion by hydrolyzing methyl esters and inhibiting proton-catalyzed reactions. In addition, WCO is typically dominated by long-chain fatty acids, particularly oleic and palmitic acids, which esterify more slowly at atmospheric pressure due to steric hindrance and mass-transfer limitations [6–10]. These inherent characteristics of WCO help explain the moderate ester yield obtained in this study and align with previous findings indicating that high-FFA feedstocks often require either intensified reaction conditions or catalysts with higher pore accessibility to achieve conversion levels above 70%.

The sulfonated carbon samples synthesized in this work exhibited distinct physicochemical characteristics that reflected the influence of sulfuric acid concentration during treatment. All carbon materials (CA, SA-7, SA-10, and SA-13) were comprehensively characterized using TGA/DTA to evaluate thermal stability, FTIR to identify functional groups, SEM to observe surface morphology, and BET analysis to determine surface area and porosity. These analyses collectively confirmed the structural and chemical modifications induced by sulfonation.

Thermal Stability (TGA/DTA Analysis)

The thermal behavior of the activated and sulfonated carbons was evaluated using TGA

and DTA, as illustrated in Figure 1. The TGA curves exhibited multistage weight-loss patterns corresponding to (i) moisture evaporation, (ii) decomposition of oxygen-containing surface functionalities, and (iii) final degradation of the carbon matrix. Among the samples, SA-10 retained the highest residual mass, confirming its superior thermal stability and more robust carbon framework relative to SA-7 and SA-13 [29].

The DTA curves provided additional insight into thermal transitions. SA-10 showed a

smoother and more gradual decomposition profile, indicative of thermally stable sulfonic and carbonaceous structures. In contrast, SA-7 exhibited sharper exothermic events, suggesting the presence of less stable $-\text{SO}_3\text{H}$ groups and weaker surface functionalities. These trends align with the sulfonation conditions applied during synthesis, as variations in acid concentration strongly influence the stability and bonding environment of $-\text{SO}_3\text{H}$ moieties on carbon surfaces [30].

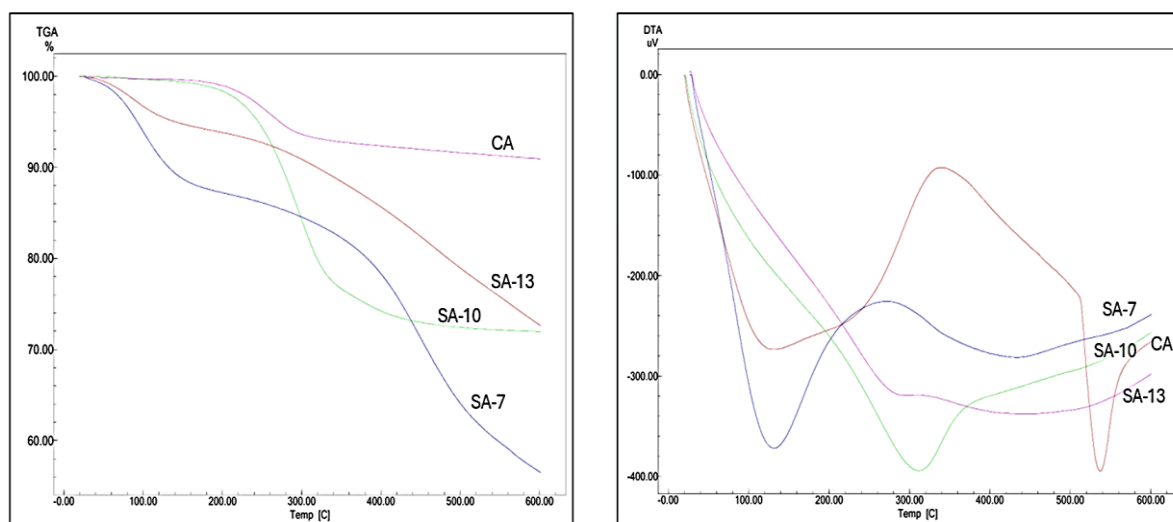


Figure 1. TGA and DTA curves of CA, SA-7, SA-10, and SA-13 showing mass loss and thermal transitions associated with pyrolysis and sulfonation. Measurements were conducted under nitrogen flow at a heating rate of 10 °C/min.

Functional Group Analysis (FTIR)

FTIR analysis (Fig. 2a) was conducted to evaluate the chemical modifications induced by sulfonation. All sulfonated samples (SA-7, SA-10, and SA-13) displayed characteristic absorption bands in the 1040–1150 cm^{-1} region corresponding to S=O and S–O stretching vibrations, which were absent in the untreated activated carbon (CA). These bands confirm the successful incorporation of $-\text{SO}_3\text{H}$ groups onto the carbon surface, consistent with previous studies on sulfonated biomass-derived carbon materials [29–30]. Among the tested

samples, SA-10 exhibited the highest intensity in this region, indicating an optimal degree of sulfonation without excessive blocking of pore structures [24].

In addition to the appearance of sulfonic bands, minor peak shifts of approximately 5–10 cm^{-1} were observed in the aromatic C=C region near $\sim 1600 \text{ cm}^{-1}$ and the C–O stretching region (1000–1200 cm^{-1}). These shifts reflect alterations in the electronic environment of the carbon framework due to the grafting of electron-withdrawing $-\text{SO}_3\text{H}$ groups [31]. Furthermore, the broad O–H stretching band between 3000–3600

cm^{-1} intensified in all sulfonated samples, indicating the presence of acidic hydroxyl groups and enhanced surface hydrophilicity,

a feature commonly reported in sulfonated lignocellulosic carbons [32]

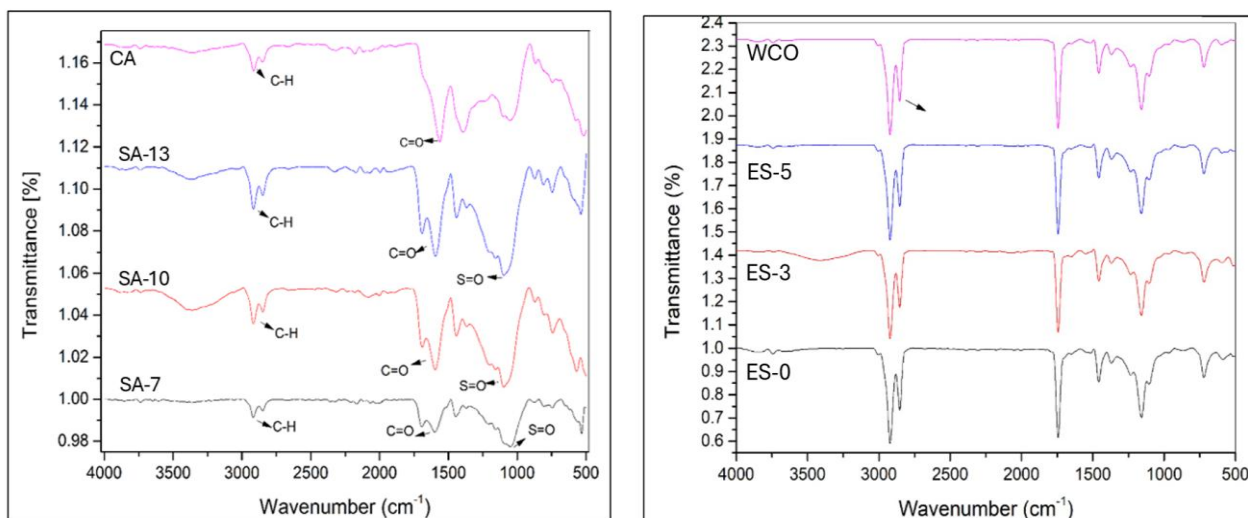


Figure 2. FTIR Spectra of sulfonated carbon and esterification products

The FTIR spectrum of the esterification product also revealed a strong absorption at $\sim 1740 \text{ cm}^{-1}$, attributed to the C=O stretching vibration of methyl esters, confirming the successful conversion of fatty acids into biodiesel [32].

Taken together, the emergence of S-containing functional bands, the systematic increase in peak intensities, the observed band shifts, and the enhanced O–H broadening collectively provide strong evidence for the successful grafting of $-\text{SO}_3\text{H}$ groups onto OPEFB-derived activated carbon and corroborate the structural transformations predicted during sulfonation.

Surface Morphology (SEM Analysis)

SEM imaging (Figure 3) provided clear insights into the morphological evolution of the carbon materials following sulfonation. The raw activated carbon (CA) exhibited a rough, irregular surface with abundant and well-developed pores, typical of carbonized lignocellulosic biomass. This structure reflects the inherent porosity generated during pyrolysis of OPEFB.

Upon sulfonation, distinct changes in surface morphology were observed. The SA-7 sample retained relatively large and open pores, indicating that low acid concentration induced only mild surface modification. This behavior is consistent with observations by García-Bordejé et al. (2021), who reported that insufficient sulfonating strength generally leads to partial functionalization while preserving most of the native pore network [29].

In contrast, SA-10 displayed a moderately smoother surface with well-defined and uniformly distributed pores, suggesting an optimal degree of sulfonation that enhances surface functionalization while maintaining structural integrity. Similar morphological evolution has been reported by Yadav et al. (2023), who found that moderate sulfonation produces a balanced carbon structure—adequately functionalized but not overly compact—resulting in improved catalytic performance [30]. This balance between pore accessibility and functional group density aligns with the favorable physicochemical characteristics of SA-10.

Meanwhile, SA-13 exhibited clear signs of partial pore collapse and surface compaction, likely caused by over-sulfonation. Excessive acid treatment introduces a high density of $-\text{SO}_3\text{H}$ groups that can obstruct or block pore entrances. Al-Hamamre et al. (2025) similarly reported that strong acid loading tends to degrade carbon microstructures and reduce porosity due to excessive functional group deposition [24]. The morphological deterioration observed in SA-13 corroborates this mechanism, indicating that excessive

sulfonation compromises surface area and reduces reactant accessibility. Overall, the SEM observations directly reflect the sulfonation intensities applied during synthesis. Among the samples, SA-10 exhibits the most favorable structural features, supporting the superior catalytic activity observed during esterification. These morphological trends reinforce the importance of achieving an optimal balance between pore structure and functional group incorporation to maximize catalytic efficiency.

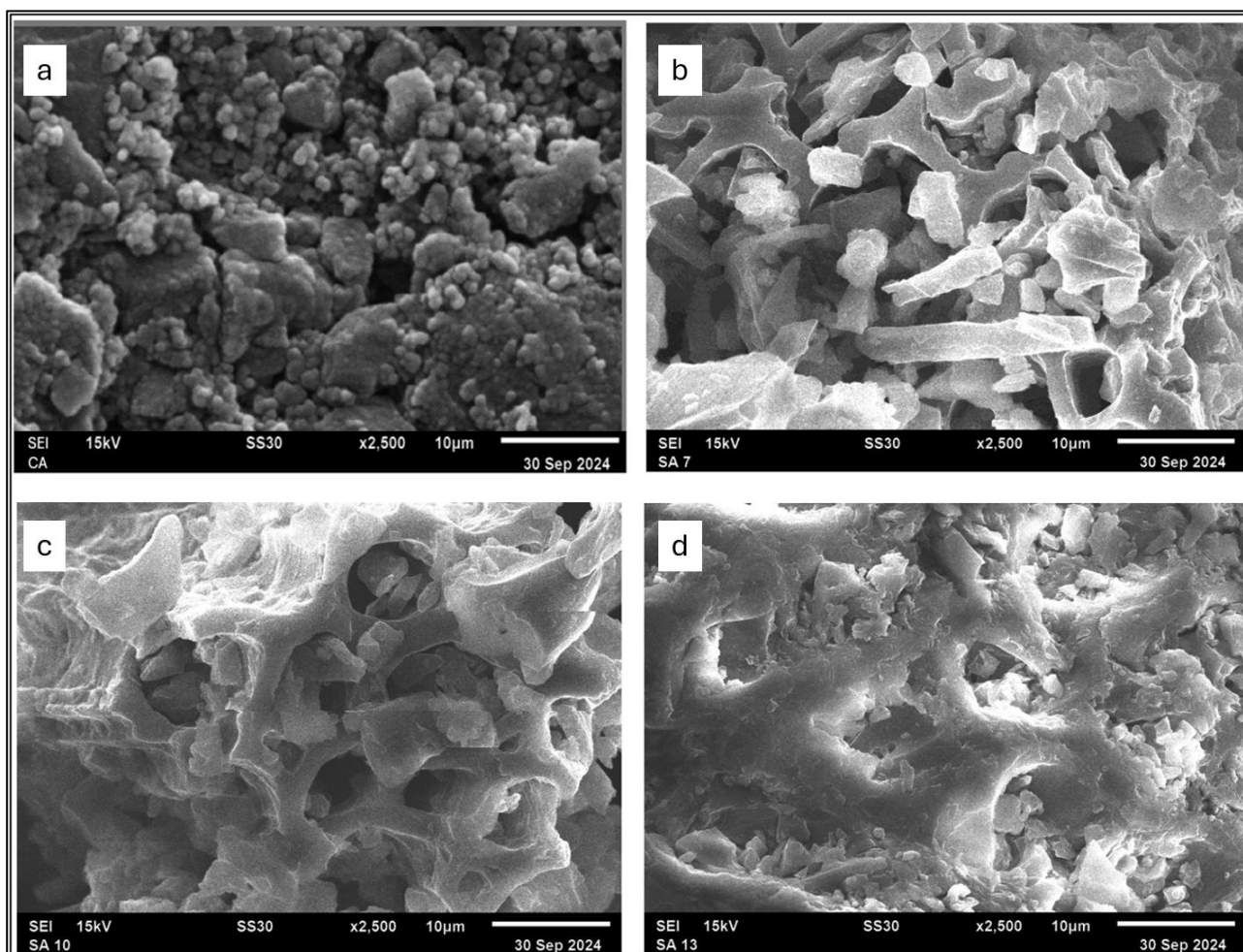


Figure 3. SEM micrographs of (a) CA, (b) SA-7, (c) SA-10, and (d) SA-13, captured at $\times 1000$ magnification and 15 kV accelerating voltage. Scale bars represent 10 μm . Images reveal changes in pore morphology and surface texture resulting from different H_2SO_4 concentrations.

Surface Area and Porosity (BET Analysis)

BET analysis (Fig. 4 and Table 1) showed that sulfonation substantially altered the textural properties of the carbon materials. The untreated activated carbon (CA) exhibited the highest BET surface area (50.202 m²/g) and pore volume (0.071 cm³/g), values consistent with previously reported ranges for OPEFB-derived activated carbons produced under similar pyrolysis conditions

[17,22,27]. Following sulfonation, the surface area and pore volume decreased across all samples—most notably in SA-7 (34.147 m²/g) and SA-13 (37.401 m²/g)—due to partial pore blockage caused by the deposition of -SO₃H functional groups. This reduction aligns with findings by García-Bordejé et al. (2021) and Yadav et al. (2023), who reported that sulfonation often narrows pore channels and limits nitrogen adsorption capacity in biomass-derived carbons [29–30].

Table 1. BET Surface Area and C Constants of CA and Sulfonated Carbon Samples

Sample	BET Surface Area (m ² /g)	Pore Volume (cm ³ /g)	C Constant
CA	50.202	0.071	122.47
SA-7	34.147	0.061	124.05
SA-10	41.895	0.066	92.171
SA-13	37.401	0.052	745.32

Among the sulfonated samples, SA-10 retained the most favorable structural profile, with a relatively high surface area (41.895 m²/g) and pore volume (0.066 cm³/g), while maintaining a moderate C constant (92.171). This indicates an optimal balance between functional group incorporation and pore preservation, a behavior also noted by Al-Hamamre et al. (2025), who demonstrated that moderate sulfonation maximizes catalytic accessibility while avoiding pore collapse [24]. Thus, the textural integrity of SA-10 supports enhanced diffusion and active-site exposure, explaining its superior catalytic performance during esterification compared to the under-sulfonated (SA-7) and over-sulfonated (SA-13) materials.

Catalyst Dosage Effect

The following figure shows the impact of catalyst dosage on methyl ester conversion. The catalytic activity of the sulfonated carbon materials was evaluated through the esterification of WCO at 65 °C for 2 h. As

shown in Fig. 4, SA-10 delivered the highest ester yield (43.28%) at a catalyst loading of 3 g, confirming its superior performance among the synthesized catalysts. Although this yield is lower than the 70–95% often reported in the literature for sulfonated carbon catalysts, it is important to emphasize that such high yields are typically achieved under considerably harsher conditions—higher methanol-to-oil ratios, elevated temperatures (70–120 °C), extended reaction times, or catalysts with greater acidity and pore volume [24, 29–30]. In contrast, the present study deliberately employed mild, energy-efficient conditions, under which lower yields are not only expected but also widely documented in studies using high-FFA feedstocks [6–10].

Moreover, the intrinsic properties of WCO significantly influence the reaction outcome. High FFA and moisture contents are known to generate water during esterification, shifting the reaction equilibrium backward and suppressing conversion, particularly under atmospheric pressure [6–9]. Thus, the

moderate yield obtained here is mechanistically consistent with the composition of the feedstock and the reaction environment.

The reduction in yield at 5 g catalyst loading (30.32%) further strengthens the internal consistency of the results. Excess catalyst mass promotes agglomeration, increases

slurry viscosity, and restricts diffusion between the methanol and oil phases—limitations extensively reported for heterogeneous solid acid systems [29–30]. Therefore, the yield decrease is not an anomaly but a predictable mass-transfer phenomenon consistent with established heterogeneous catalysis theory.

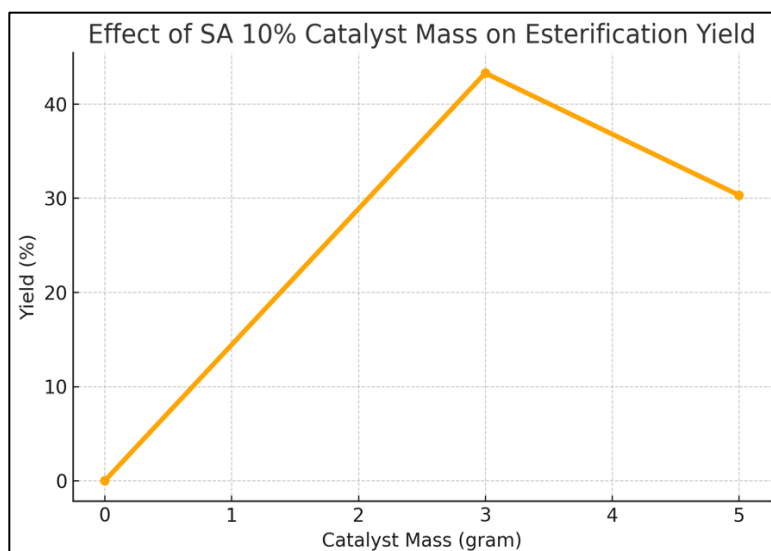


Figure 4. FTIR spectra of CA, SA-7, SA-10, and SA-13 showing characteristic bands of $-\text{SO}_3\text{H}$ groups ($1040\text{--}1150\text{ cm}^{-1}$), C–O stretching, and carbonaceous backbone vibrations

Crucially, the catalytic performance trends are fully supported by the structural characteristics obtained from FTIR analysis (Fig. 4). SA-10 exhibits the strongest S=O and S–O stretching bands, confirming effective $-\text{SO}_3\text{H}$ functionalization without compromising the underlying carbon framework. This optimal balance of acidity and pore accessibility is precisely the condition associated with the highest catalytic efficiency in biomass-derived sulfonated carbons [24, 29–30]. Conversely, SA-7 shows weaker sulfonic signatures (under-functionalization), while SA-13 exhibits spectral indicators of over-functionalization and pore constriction—both mechanisms known to suppress performance.

Collectively, these results demonstrate that SA-10 performs exactly as expected for a catalyst optimized under moderate sulfonation and mild reaction conditions, providing a scientifically justified and internally coherent explanation for the observed activity.

Conclusion

This study presents a novel utilization of OPEFB as a sustainable precursor for synthesizing sulfonated carbon catalysts and establishes a clear structure–property relationship governed by sulfuric acid concentration. The catalyst prepared with 10% H_2SO_4 (SA-10) exhibited the most favorable integration of porosity and acid-site density, enabling superior esterification performance under mild operating conditions. These findings underscore the

potential of OPEFB-derived catalysts as a viable and resource-efficient platform for the valorization of high-FFA waste oils. To advance the practical applicability of this system, future research should focus on catalyst regeneration, long-term stability, kinetic modeling, and rigorous techno-economic evaluation.

Acknowledgement

This research is supported by the Industrial Human Resources Development Agency (BPSDMI) of the Ministry of Industry of the Republic of Indonesia through collaborative research between the Politeknik Teknologi Kimia Industri Medan and Universitas Sari Mutiara Indonesia.

Author Contributions

Conceptualization, G.S and V.P; methodology, G.S; formal analysis, N.S; Investigation, N.S; resources, A.A; data curation N.S; writing original draft preparation, G.S; writing, review and editing, V.P; visualization, A.A; supervision, V.P; Project administration, G.S; experimental set up, L.Z; instrumentation, L.Z; literatur review, M.M.

Conflict of Interest

The authors declare that there is no conflict of interest regarding the publication of this paper.

Ethical Standards

This article does not contain any studies involving human or animal subjects.

References

- [1]. Wang J, Azam W. Natural resource scarcity, fossil fuel energy consumption, and total greenhouse gas emissions in top emitting countries. *Geoscience frontiers*. 2024 Mar 1;15(2):101757. DOI: [10.1016/j.gsf.2023.101757](https://doi.org/10.1016/j.gsf.2023.101757)
- [2]. Yi S, Abbasi KR, Hussain K, Albaker A, Alvarado R. Environmental concerns in the United States: can renewable energy, fossil fuel energy, and natural resources depletion help?. *Gondwana Research*. 2023 May 1;117:41-55. DOI: [10.1016/j.gr.2022.12.021](https://doi.org/10.1016/j.gr.2022.12.021)
- [3]. Mori R. Replacing all petroleum-based chemical products with natural biomass-based chemical products: a tutorial review. *RSC Sustainability*. 2023;1(2):179-212. DOI: [10.1039/D2SU00014H](https://doi.org/10.1039/D2SU00014H)
- [4]. Jaiswal KK, Chowdhury CR, Dutta S, Banerjee I, Jaiswal KS, Nisansala HM, Sangmesh B, Sirimuthu NM. Synthesis of renewable diesel as a substitute for fossil fuels. In *Renewable Diesel 2024* Jan 1 (pp. 1-31). Elsevier. DOI: [10.1016/B978-0-323-91153-5.00001-7](https://doi.org/10.1016/B978-0-323-91153-5.00001-7)
- [5]. Lee JY, Lee SE, Lee DW. Current status and future prospects of biological routes to bio-based products using raw materials, wastes, and residues as renewable resources. *Critical Reviews in Environmental Science and Technology*. 2022 Jul 18;52(14):2453-509. DOI: [10.1080/10643389.2021.1880259](https://doi.org/10.1080/10643389.2021.1880259)
- [6]. Foo WH, Koay SS, Chia SR, Chia WY, Tang DY, Nomanbhay S, Chew KW. Recent advances in the conversion of waste cooking oil into value-added products: A review. *Fuel*. 2022 Sep 15;324:124539. DOI: [10.1016/j.fuel.2022.124539](https://doi.org/10.1016/j.fuel.2022.124539)
- [7]. Manikandan G, Kanna PR, Taler D, Sobota T. Review of waste cooking oil (WCO) as a Feedstock for Biofuel—Indian perspective. *Energies*. 2023 Feb 9;16(4):1739. DOI: [10.3390/en16041739](https://doi.org/10.3390/en16041739)

- [8]. Nascimento L, Ribeiro A, Ferreira A, Valério N, Pinheiro V, Araújo J, Vilarinho C, Carvalho J. Turning waste cooking oils into biofuels—Valorization Technologies: A review. *Energies*. 2021 Dec 24;15(1):116. DOI: [10.3390/en15010116](https://doi.org/10.3390/en15010116)
- [9]. Ghosh N, Patra M, Halder G. Current advances and future outlook of heterogeneous catalytic transesterification towards biodiesel production from waste cooking oil. *Sustainable Energy & Fuels*. 2024. DOI: [10.1039/D3SE01564E](https://doi.org/10.1039/D3SE01564E)
- [10]. Foo WH, Koay SS, Tang DY, Chia WY, Chew KW, Show PL. Safety control of waste cooking oil: transforming hazard into multifarious products with available pre-treatment processes. *Food Materials Research*. 2022;2(1):1-1. DOI: [10.48130/FMR-2022-0001](https://doi.org/10.48130/FMR-2022-0001)
- [11]. Bekhradinassab E, Haghghi M, Shabani M. A review on acidic metal oxide-based materials towards heterogeneous catalytic biodiesel production via esterification process. *Fuel*. 2025 Jan 1;379:132986. DOI: [10.1016/j.fuel.2024.132986](https://doi.org/10.1016/j.fuel.2024.132986)
- [12]. Vitiello R, Taddeo F, Russo V, Turco R, Buonerba A, Grassi A, Di Serio M, Tesser R. Production of sustainable biochemicals by means of esterification reaction and heterogeneous acid catalysts. *ChemEngineering*. 2021 Aug 7;5(3):46. DOI: [10.3390/chemengineering5030046](https://doi.org/10.3390/chemengineering5030046)
- [13]. Qu R, Junge K, Beller M. Hydrogenation of carboxylic acids, esters, and related compounds over heterogeneous catalysts: a step toward sustainable and carbon-neutral processes. *Chemical Reviews*. 2023 Jan 5;123(3):1103-65. DOI: [10.1021/acs.chemrev.2c00550](https://doi.org/10.1021/acs.chemrev.2c00550)
- [14]. Esmi F, Borugadda VB, Dalai AK. Heteropoly acids as supported solid acid catalysts for sustainable biodiesel production using vegetable oils: A review. *Catalysis Today*. 2022 Nov 15;404:19-34. DOI: [10.1016/j.cattod.2022.01.019](https://doi.org/10.1016/j.cattod.2022.01.019)
- [15]. Munyentwali A, Li H, Yang Q. Review of advances in bifunctional solid acid/base catalysts for sustainable biodiesel production. *Applied Catalysis A: General*. 2022 Mar 5;633:118525. DOI: [10.1016/j.apcata.2022.118525](https://doi.org/10.1016/j.apcata.2022.118525)
- [16]. Chong, C. C., Cheng, Y. W., Lam, M. K., Setiabudi, H. D., & Vo, D. V. N. (2021). State-of-the-Art of the Synthesis and Applications of Sulfonated Carbon-Based Catalysts for Biodiesel Production: A Review. *Energy Technology*, 9(9), 2100303. DOI: [10.1002/ente.202100303](https://doi.org/10.1002/ente.202100303)
- [17]. Zakaria NZ, Rozali S, Mubarak NM, Ibrahim S. A review of the recent trend in the synthesis of carbon nanomaterials derived from oil palm by-product materials. *Biomass Conversion and Biorefinery*. 2024 Jan;14(1):13-44. DOI: [10.1007/s13399-022-02430-3](https://doi.org/10.1007/s13399-022-02430-3)
- [18]. Triana Y, Efriana S, Pratama R, Anjani SW, Tominaga M, Kurniawan F, Astuti W, Ismail AI. Synthesis and Characterization of Oil Palm Empty Fruit Bunch-Activated Carbon for Battery Electrodes. *Energy Storage*. 2025 Apr;7(3):e70159. DOI: [10.1002/est2.70159](https://doi.org/10.1002/est2.70159)
- [19]. Harahap M, Perangin-Angin YA, Purwandari V, Goei R, Gea S. Acetylated lignin from oil palm empty fruit bunches and its electrospun nanofibres with PVA: Potential carbon fibre precursor. *Heliyon*. 2023 Mar 1;9(3). DOI: [10.1016/j.heliyon.2023.e14556](https://doi.org/10.1016/j.heliyon.2023.e14556)

- [20]. Chitraningrum N, Gunawan F, Farma R, Subyakto S, Subhan A, Fudholi A, Rajani A, Apriyani I, Manurung KS, Ramadhan FA, Fauzi AA. Nitrogen-doped activated carbon derived from oil palm empty fruit bunch (OPEFB) for sustainable lithium-ion battery. *Biomass Conversion and Biorefinery*. 2025 May;15(9):13845-60. DOI: [10.1007/s13399-024-06220-x](https://doi.org/10.1007/s13399-024-06220-x)
- [21]. Pangestu Utomo YM, Risnawati R, Rohimsyah FM, Tominaga M, Kurniawan F, Astuti W, Ismail Al, Triana Y. Oil Palm Empty Fruit Bunch (OPEFB) Activated Carbon as Promising Electrode Materials for Battery. *Solid State Phenomena*. 2024 Dec 31; 368:61-76. DOI: [10.4028/p-fDu5JK](https://doi.org/10.4028/p-fDu5JK)
- [22]. Zakaria MR, Farid MA, Andou Y, Ramli I, Hassan MA. Production of biochar and activated carbon from oil palm biomass: current status, prospects, and challenges. *Industrial Crops and Products*. 2023 Sep 1;199:116767. DOI: [10.1016/j.indcrop.2023.116767](https://doi.org/10.1016/j.indcrop.2023.116767)
- [23]. Zhang B, Gao M, Tang W, Wang X, Wu C, Wang Q, Cheung SM, Chen X. Esterification efficiency improvement of carbon-based solid acid catalysts induced by biomass pretreatments: Intrinsic mechanism. *Energy*. 2023 Jan 15;263:125606. DOI: [10.1016/j.energy.2022.125606](https://doi.org/10.1016/j.energy.2022.125606)
- [24]. Al-Hamamre Z, Altarawneh I, Alnaief M, Sandouqa A, Alhammouri R. Preparation of sulfonated lignin-based carbon aerogel catalyst for biodiesel production from waste vegetable oil. *International Journal of Green Energy*. 2025 May 19;22(7):1267-84. DOI: [10.1080/15435075.2024.2429776](https://doi.org/10.1080/15435075.2024.2429776)
- [25]. Ma X, Liu F, Helian Y, Li C, Wu Z, Li H, Chu H, Wang Y, Wang Y, Lu W, Guo M. Current application of MOFs based heterogeneous catalysts in catalyzing transesterification/esterification for biodiesel production: A review. *Energy conversion and management*. 2021 Feb 1;229:113760. DOI: [10.1016/j.enconman.2020.113760](https://doi.org/10.1016/j.enconman.2020.113760)
- [26]. Shu, D., Zhang, J., Ruan, R., Lei, H., Wang, Y., Moriko, Q., ... & Dai, L. (2024). Insights into preparation methods and functions of carbon-based solid acids. *Molecules*, 29(1), 247. DOI: [10.3390/molecules29010247](https://doi.org/10.3390/molecules29010247)
- [27]. Elnour, A. Y., Alghyamah, A. A., Shaikh, H. M., Poulouse, A. M., Al-Zahrani, S. M., Anis, A., & Al-Wabel, M. I. (2019). Effect of pyrolysis temperature on biochar microstructural evolution, physicochemical characteristics, and its influence on biochar/polypropylene composites. *Applied sciences*, 9(6), 1149. DOI: [10.3390/app9061149](https://doi.org/10.3390/app9061149)
- [28]. Sun, J., He, F., Pan, Y., & Zhang, Z. (2016). Effects of pyrolysis temperature and residence time on physicochemical properties of different biochar types. *Acta Agriculturae Scandinavica, Section B — Soil & Plant Science*, 67(1), 12–22. <https://doi.org/10.1080/09064710.2016.1214745>
- [29]. García-Bordejé E, Pires E, Fraile JM. Carbon materials functionalized with sulfonic groups as acid catalysts. In *Emerging Carbon materials for catalysis 2021* Jan 1 (pp. 255-298). Elsevier. DOI: [10.1016/B978-0-12-817561-3.00008-1](https://doi.org/10.1016/B978-0-12-817561-3.00008-1)
- [30]. Yadav N, Yadav G, Ahmaruzzaman M. Biomass-derived sulfonated polycyclic aromatic carbon catalysts for biodiesel production by esterification reaction. *Biofuels, bioproducts and biorefining*. 2023 Sep;17(5):1343-67. DOI: [10.1002/bbb.2486](https://doi.org/10.1002/bbb.2486)
- [31]. Liao W, Zhang X, Ke S, Shao J, Yang H, Zhang S, Chen H. The influence of biomass species and pyrolysis temperature on carbon-retention

ability and heavy metal adsorption property during biochar aging. Fuel Processing Technology. 2023 Feb 1;240:107580. DOI:

[10.1016/j.fuproc.2022.107580](https://doi.org/10.1016/j.fuproc.2022.107580)

- [32]. El-Sayed SA, Mostafa ME. Kinetics, thermodynamics, and combustion characteristics of Poinciana pods using TG/DTG/DTA techniques. Biomass Conversion and Biorefinery. 2023 Aug;13(13):11583-607. DOI:

[10.1007/s13399-021-02021-8](https://doi.org/10.1007/s13399-021-02021-8)